Available online at www.sciencedirect.com

ScienceDirect

Journal of the European Ceramic Society 32 (2012) 1447–1455

www.elsevier.com/locate/jeurceramsoc

Characterization investigations of ZrB_2/ZrC ceramic powders synthesized by mechanical alloying of elemental Zr, B and C blends

Duygu Ağaoğulları *, Hasan Gökçe, İsmail Duman, M. Lütfi Öveçoğlu

Istanbul Technical University, Faculty of Chemical and Metallurgical Engineering, Department of Metallurgical and Materials Engineering,
Ayazağa Campus, 34469 Maslak, Istanbul, Turkey

Abstract

ZrB_2/ZrC ceramic powders were fabricated by mechanical alloying (MA) of zirconium (Zr), amorphous boron (B) and graphite (C) powder blends prepared in the mole ratios of Zr/B/C: 1/1/1, 1/2/1, 1/1/2, 1/2/2 and 2/2/1. MA runs were carried out in a vibratory ball mill using hardened steel vial/balls. The effects of Zr/B/C mole ratios and milling duration on the formation and microstructure of ZrB_2/ZrC ceramic powders were examined. Gibbs free energy change-temperature relations of the reactions and moles of the products were interpreted by thermochemical software. Zr/B/C: 1/1/1, 1/2/1, 1/1/2 and 1/2/2 powder blends MA'd for 2 and 3 h contain unreacted Zr and C, ZrB_2, ZrC and B_4C particles. Synthesis of ZrB_2/ZrC ceramic powders was completely accomplished after MA of Zr/B/C: 2/2/1 powder blend for 2 h. ZrC and ZrB_2 particles were obtained ranging in size between 50 and 250 nm in the presence of FeB contamination (<1 wt.%).

Keywords: Solid state reaction; Mechanical alloying; Ceramic powders; Carbides; Borides

1. Introduction

Zirconium diboride (ZrB_2) is a IVB Group transition metal boride classified as a high-temperature advanced ceramic material. Owing to its high melting point, high hardness, high elastic modulus, good electrical conductivity and excellent thermal shock resistance, ZrB_2 is a potential candidate material for high performance applications. Moreover, it has high resistance to oxidation at elevated temperatures and excellent chemical resistance to HCl, HF, molten metals (Al, Cu, Mg, Zn, Cd, Fe, Pb), cryolite and non-basic slags.[1,2] Concerning these properties, ZrB_2 has been used in thermal protection systems for hypersonic flight, atmospheric re-entry and rocket propulsion and in other high-temperature applications including evaporation boats, crucibles for handling molten metals, thermowells, thermocouple sieves, wear parts, nozzles, armours, cutting tools and cathodes for electrochemical processing of aluminium.[1–5] It has also been utilized as dispersoid in metal and ceramic composites for improving mechanical properties.[3–5] Several techniques, such as fused-salt electrolysis, carbothermic and borothermic reduction, gas phase combustion synthesis, solution phase processing and self-propagating high-temperature synthesis (SHS), have been established to produce ZrB_2 powders.[1–5]

Zirconium carbide (ZrC) is an ultra high temperature ceramic (UHTC) having a number of superior properties such as high melting point, high hardness, high strength, good thermal shock resistance, high thermal and electrical conductivity, low evaporation rate, solid-state phase stability and neutron transparency.[6,7] Differing from ZrB_2, ZrC has potential uses in field emission arrays, microwave devices, spacecraft charge dissipation devices, diffusion barrier coatings on UO_2 particles in nuclear industry, manufacture of electrodes, filaments, refractory parts and protective shields of metallic thermocouples.[7,8]

The use of ZrB_2 and ZrC ceramics in composites can be expected to offer potential candidates for a variety of high-temperature thermal and structural applications than those exhibited separately. Due to improved mechanical properties, it is important to prepare ZrB_2/ZrC ceramic powders with fine and homogeneous structure as precursors of composites.[9–11]

Currently, there exists a number of research investigations concerning ZrB_2/ZrC composites fabricated by using different production techniques such as mechanical activation assisted self-propagating high-temperature synthesis of powder blends in molar ratio of Zr/B/C: 1/1/1–6/10/1 and spark plasma sinter-

---

* Corresponding author. Tel.: +90 212 285 6893; fax: +90 212 285 3427.
E-mail addresses: bozkurtdu@itu.edu.tr (D. Ağaoğulları), gokceh@itu.edu.tr (H. Gökçe), iduman@itu.edu.tr (İ. Duman), ovecoglu@itu.edu.tr (M.L. Öveçoğlu).

0955-2219/$ – see front matter © 2011 Elsevier Ltd. All rights reserved.
doi:10.1016/j.jeurceramsoc.2011.04.026

ing (SPS) at 1800 °C for 5–10 min under vacuum at a pressure of 40 MPa.[9–11] Ultra-fine ZrB_2/ZrC composite powders have been synthesized by a sol–gel method using zirconium oxychloride, boric acid and phenolic resin as sources of zirconia, boron oxide and carbon, respectively.[12] Powders have been also produced by boro/carbothermal reduction of zirconium dioxide, boron carbide and carbon at 1650 °C after 1 h in a vacuum atmosphere.[13] Furthermore, dense ZrB_2/ZrC and $ZrB_2/ZrC_{x-0.67}$ composites have been achieved by reactive hot pressing (RHP) of stoichiometric and non-stoichiometric blends of Zr and B_4C powders at 1600 °C for 30 min at a pressure of 40 MPa.[14] A study concerning spark plasma sintering of ZrB_2/ZrC_x composites from commercial powders has been realized considering the effects of applied load, temperature and heating duration.[15,16] Moreover, dense ZrB_2/ZrC/Zr composites have been fabricated via reaction sintering of molten Zr with ZrB_2 preform and infiltration of molten Zr into ZrB_2 preform which contains 0–40 vol.% B_4C, at 1900 °C for 10 min.[17]

In previous studies, ZrB_2/ZrC composites have been commonly prepared by using high-temperature fabrication techniques. However, room temperature production route of ZrB_2/ZrC ceramic powders is not a well-discussed topic. Consequently, solid-state reaction of powder particles named as mechanical alloying can be used as an alternative method without need of high-temperatures.

Mechanical alloying (MA) is a high-energy ball milling technique utilizing various types of mills in which a mixture of different powders is subjected to highly energetic compressive forces. By the repeated fracture and cold welding of the constituent powder particles, it is possible to make alloys from normally immiscible components. Due to the fact that it is a simple method to synthesize the nanocrystalline materials at room temperature, it has been recently used to synthesize the metal carbides, borides and silicides.[8,18] MA is beneficial over the other methods by means of its low cost, simplicity and high throughput. It has been also reported that carbide and/or boride powders with fine microstructures fabricated by mechanical alloying and subsequent hot pressing have exhibited desirable mechanical properties at room and elevated temperatures.[18,19]

In the present study, ZrB_2/ZrC ceramic powders were fabricated via MA in the mole ratios of Zr/B/C: 1/1/1, 1/2/1, 1/1/2, 1/2/2 and 2/2/1. The effects of MA duration and Zr/B/C mole ratios on the compositional and the microstructural features of the ceramic powders were evaluated.

2. Experimental procedure

Elemental zirconium (Zr) powders (ABCR™, 99.5% purity, 4 μm average particle size), amorphous boron powders (B) (ABCR™, 95–97%, 50 μm average particle size) and graphite powders (Alfa Aesar™, 99% purity, 45 μm average particle size) were mixed to constitute the compositions in the mole ratios of Zr/B/C: 1/1/1, 1/2/1, 1/1/2, 1/2/2 and 2/2/1. The amounts of prepared powder batches weighed in a XB320 M (Precisa™, Dietikon, Switzerland) sensitive balance were 5–6 g. MA experiments were carried out in a vibratory ball mill (Spex™ 8000 D Mixer/Mill, New Jersey, USA) using hardened steel balls (6 mm diameter) in a hardened steel vial (50 ml capacity) with a ball-to-powder weight ratio (BPR) of 10:1. Milling was performed with a lower BPR with the intention of obtaining fine pulverization, large contact surface, short reaction time and high efficiency. Milling vials were evacuated to about 10^{-2} Pa and then sealed in a glove box (Plaslabs™, Michigan, USA) under Ar gas (Linde™, 99.999% purity) to prevent surface oxidation and contamination of powder blends from atmospheric conditions. MA durations varied from 30 min to 3 h. Extended durations were not preferred due to possibility of the formations of intermetallic phases other than ZrB_2 and ZrC. Milling was not interrupted and at the end of mentioned durations, mechanically alloyed (MA'd) powders were unloaded again under Ar atmosphere in the glove-box. Additionally, as-blended (non-MA'd) Zr/B/C powders were mixed and homogenized in a T2C Turbula (WAB™, Basel, Switzerland) blender for 2 h.

The phase compositions of the MA'd powders were performed by X-ray diffraction (XRD) technique using a D8 Advanced Series Powder Diffractometer (Bruker™, Karlsruhe, Germany) with CuKα (1.54060 Å) radiation in the 2θ range of 20–100° with 0.02° steps at a rate of 2°/min. International Centre for Diffraction Data® (ICDD) powder diffraction files were utilized for the identification of crystalline phases. Microstructural characterizations of the MA'd powders were carried out using a JSM-7000F (Jeol™, Tokyo, Japan) scanning electron microscope/energy dispersive spectrometer (SEM/EDS) operated at 10 kV and using a JEM-2000EX (Jeol™, Tokyo, Japan) transmission electron microscope (TEM) operated at 160 kV. In order to determine both residual elements and approximate formation temperatures of ZrB_2 and ZrC phases, as-blended and 2 h MA'd Zr/B/C: 2/2/1 powders were placed in alumina boats and heated in a PTF 16/75/450 (Protherm™, Ankara, Turkey) tube furnace for 1 h up to 1200 °C with a heating and cooling rate of 10 °C/min under Ar gas flow rate of 2000 ml/min. Gibbs free energy change-temperature relations of the reactions and mole ratios of the products varied according to the mole ratios of the reactants were interpreted by HSC Chemistry™ Ver. 4.1 and FactSage™ programs, respectively.

3. Results and discussion

Fig. 1 illustrates the XRD patterns of the Zr/B/C powder blends in the mole ratio of 1/1/1 after MA for 30 min, 1 h, 2 h and 3 h. It is evident from Fig. 1(a) and (b) that there is no reaction between Zr, B and C particles after milling for 30 min and 1 h since Zr (ICDD Card No: 05-0665, Bravais lattice: primitive hexagonal, $a = b = 0.323$ nm, $c = 0.515$ nm) phase is still present in the powder blends. Boron and graphite peaks cannot be seen in the XRD patterns of the Zr/B/C: 1/1/1 powders MA'd for 30 min and 1 h. The absence of boron peaks is due to its amorphous nature. Likewise, graphite powder which has small weight percentage in the total powder blend was exposed to continuous amorphization during milling. It is obvious from Fig. 1(a)–(d) that Zr peaks decreased in intensity and broadened with increasing milling duration. Continuous deformation of powder particles during milling results in crystallite refinement and increase in lattice strain.[8,10,18] As seen in Fig. 1(c), a

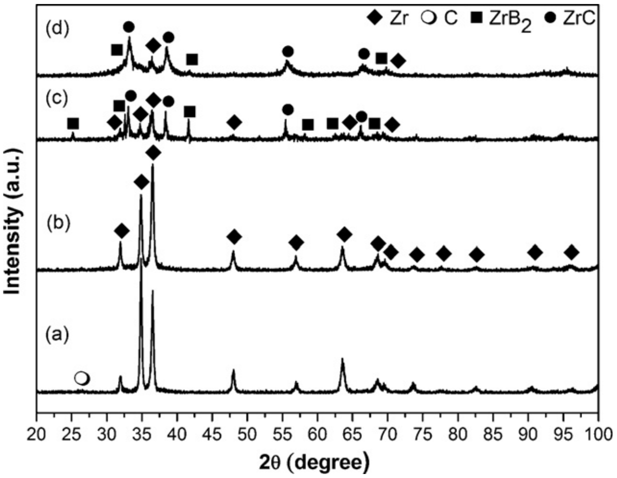

Fig. 1. XRD patterns of the Zr/B/C powder blends in the mole ratio of 1/1/1 MA'd for: (a) 30 min, (b) 1 h, (c) 2 h and (d) 3 h.

reaction takes place between particles of Zr/B/C: 1/1/1 powder blend after milling for 2 h. ZrC (ICDD Card No: 74-1221, Bravais lattice: face-centered cubic, $a = b = c = 0.476$ nm) and ZrB_2 (ICDD Card No: 34-0423, Bravais lattice: primitive hexagonal, $a = b = 0.317$ nm, $c = 0.353$ nm) phases occurred in the presence of small amount of unreacted Zr powders. The milling duration was extended to 3 h in order to observe chemical changes in the powder blend, but this change comes out as reduction in the crystallite size of ZrC and ZrB_2 particles and decrease in the amount of unreacted Zr powders (Fig. 1(d)).

Fig. 2 shows the XRD patterns of the Zr/B/C powder blends in the mole ratio of 2/2/1 after MA for 30 min, 1 h and 2 h. The mole ratio 2/2/1 was chosen as the stoichiometric amount of the powders for the complete conversion of Zr, B and C reactants to ZrB_2 and ZrC products. Similar to the Zr/B/C: 1/1/1 powder blend, no reaction occurs after milling for 30 min (Fig. 2(a)). ZrB_2 and ZrC phases form in the Zr/B/C: 2/2/1 powder blend MA'd for 1 h (Fig. 2(b)). However, there is very small amount of unreacted Zr powders. As indicated in Fig. 2(c), MA for 2 h enables a complete solid-state chemical reaction of raw materials to the reaction products containing no unreacted Zr powders. In comparison with Fig. 1(b) and (c), it can be stated that the increase of Zr/B/C molar ratio from 1/1/1 to 2/2/1 substantially changes the reaction products even if MA duration is fixed.

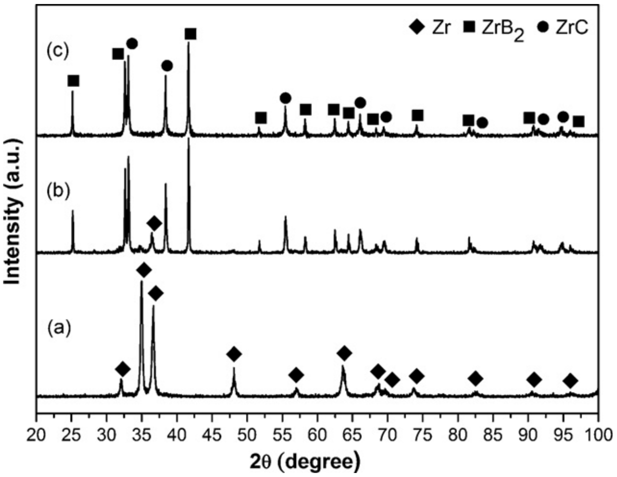

Fig. 2. XRD patterns of the Zr/B/C powder blends in the mole ratio of 2/2/1 MA'd for: (a) 30 min, (b) 1 h and (c) 2 h.

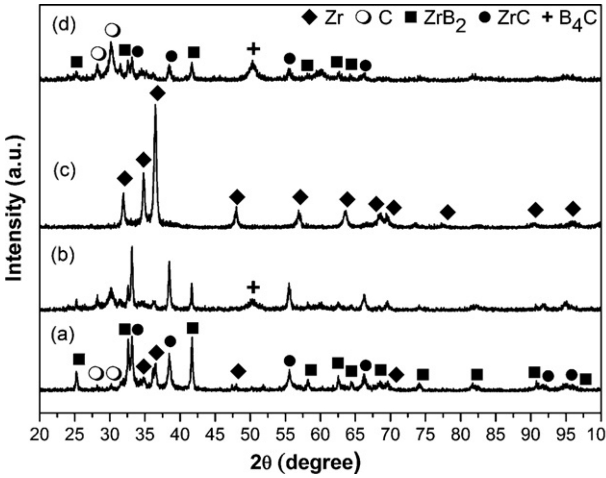

Fig. 3. XRD patterns of the Zr/B/C powder blends in the mole ratios of: (a) 1/2/1 MA'd for 2 h, (b) 1/1/2 MA'd for 2 h, (c) 1/2/2 MA'd for 2 h and (d) 1/2/2 MA'd for 3 h.

Tsuchida and Yamamoto[10] have reported that ZrB_2 and ZrC particles can be prepared from Zr/B/C: 1/1/1 powder blends by mechanical activation (for 45 min) and subsequent self-propagating high-temperature synthesis in air. Their XRD results showing only Zr peaks after MA for 45 min are in good agreement with those of this study. However, the sample is exposed to air immediately after milling and self-ignited for obtaining ZrB_2 and ZrC particles in the mentioned literature.[10] In the present study, reaction occurs at room temperature only by the repeated welding, fracturing and rewelding of powder particles of the reactant materials with a maximum MA duration of 3 h. A number of contact points are produced between the powder particles due to a reduction in particle size. This allows fresh Zr, B and C surfaces to come into contact repeatedly and thereby a solid-state reaction takes place by the conversion of mechanical energy into thermal and chemical energy which develops displacement or redox reactions. Reactions which normally require high temperatures occur at lower temperatures during MA inside the milling vial without any externally applied heat.[8,18,19]

Fig. 3(a)–(d) shows the XRD patterns of the Zr/B/C powder blends in the mole ratios of 1/2/1, 1/1/2 and 1/2/2 after MA for 2 and 3 h. ZrB_2 and ZrC phases occur in the presence of very small amount of unreacted Zr and C (ICDD Card No: 89-8494, Bravais lattice: primitive orthorhombic, $a = 0.413$ nm, $b = 0.494$ nm, $c = 0.482$ nm) in the powder blend of Zr/B/C: 1/2/1 after MA for 2 h (Fig. 3(a)). As compared with the XRD patterns in Figs. 1(c) and 2(c), the consumption of Zr particles is ordinarily expected when 2 moles of boron and 1 mole of graphite powders are used in the mixture. Though the increase in boron content (from mole ratio of B/Zr: 1/1 to B/Zr: 2/1) partially prevents the Zr and C particles to come into contact and leave behind unreacted Zr and C powders (Fig. 3(a)). As seen

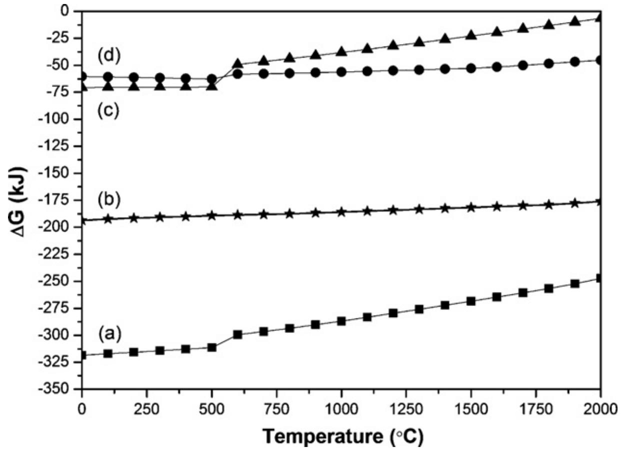

Fig. 4. Gibbs free energy change-temperature relations of the predicted reactions: (a) $Zr + 2B \rightarrow ZrB_2$, (b) $Zr + C \rightarrow ZrC$, (c) $4B + C \rightarrow B_4C$ and (d) $Fe + B \rightarrow FeB$.

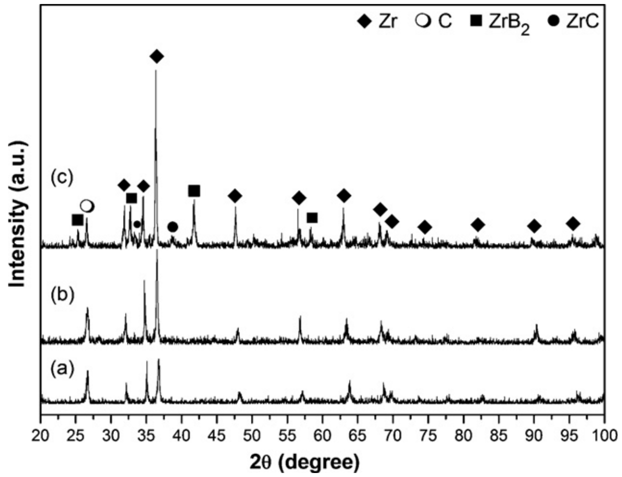

Fig. 5. XRD patterns of the as-blended Zr/B/C: 2/2/1 powders heated to: (a) 800 °C, (b) 1000 °C and (c) 1200 °C.

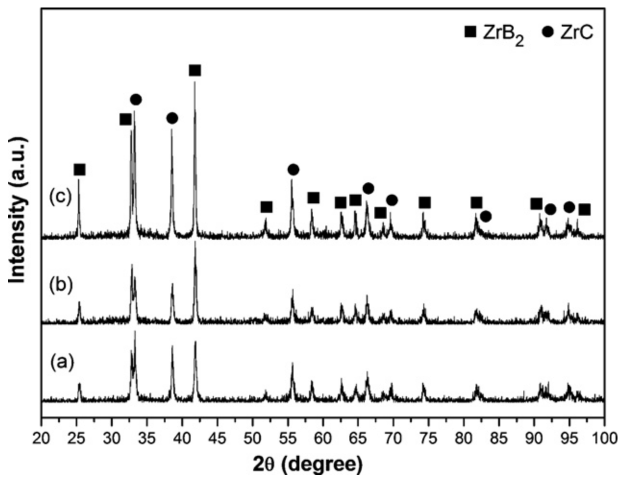

Fig. 6. XRD patterns of the Zr/B/C: 2/2/1 powder blends MA'd for 2 h and heated to: (a) 800 °C, (b) 1000 °C and (c) 1200 °C.

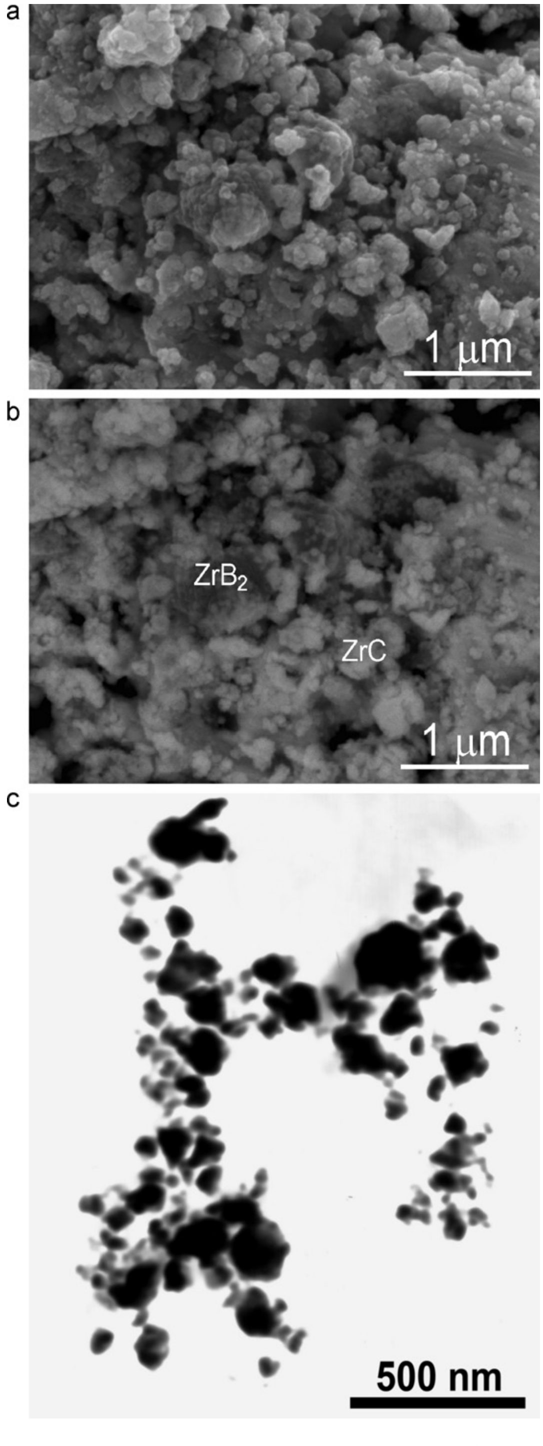

Fig. 7. Micrographs of the Zr/B/C: 2/2/1 powder blends MA'd for 2 h: (a) SEM micrograph recorded with the secondary electron detector, (b) SEM micrograph recorded with the back-scattered electron detector, (c) bright-field (BF) TEM micrograph.

in Fig. 3(b), 2 h MA'd Zr/B/C: 1/1/2 powder blend has the same phases in addition to B_4C (ICDD Card No: 75-0424, Bravais lattice: primitive rhombohedral, $a = b = 0.562$ nm, $c = 1.214$ nm). Zr/B/C: 1/2/2 powder blend which contains the least Zr, has only Zr peaks after 2 h milling (Fig. 3(c)) and has intense B_4C and unreacted graphite peaks together with ZrB_2 and ZrC after MA for 3 h (Fig. 3(d)). Thereby, undesired B_4C phase occurs when

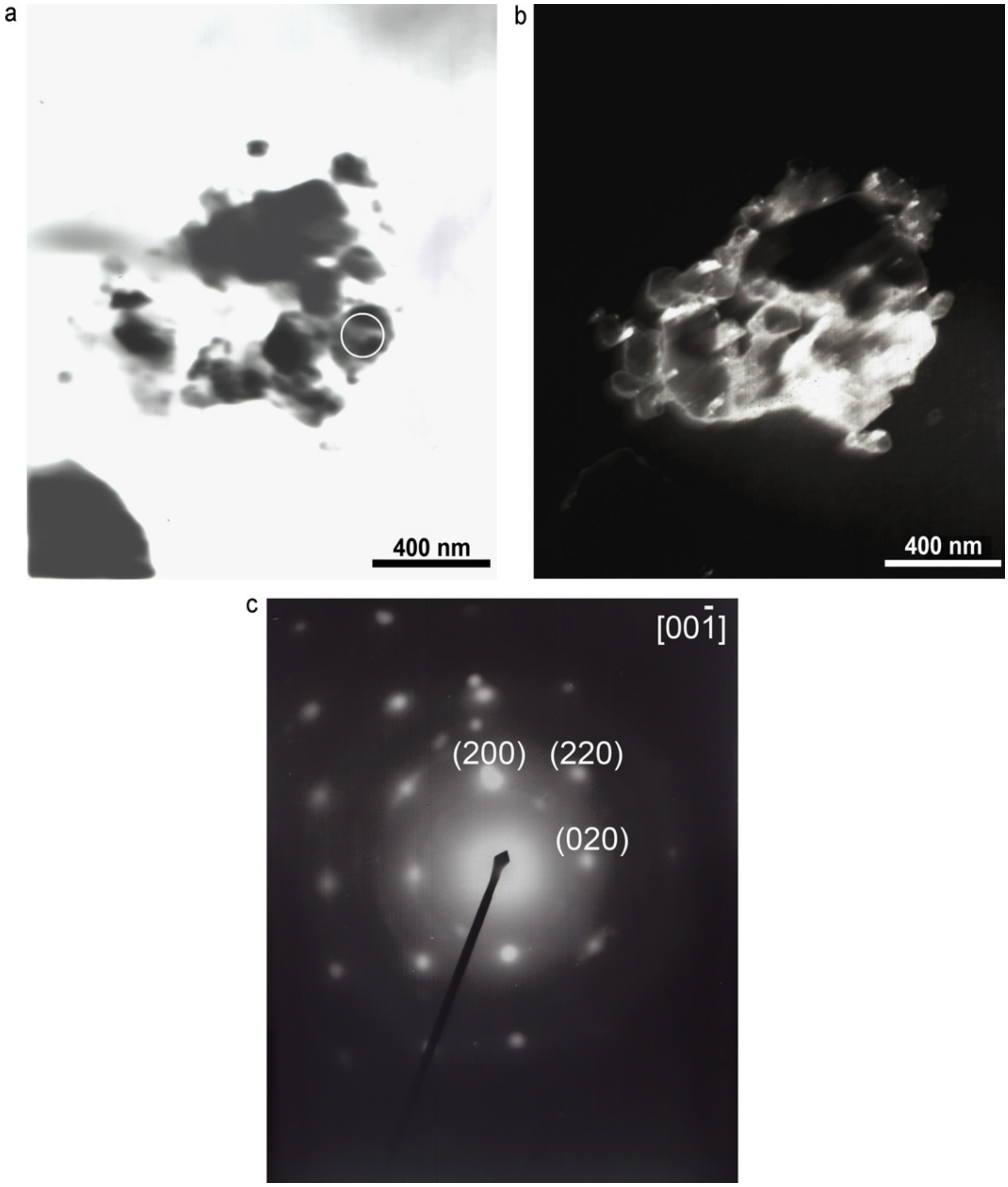

Fig. 8. TEM micrographs taken from an agglomerate of Zr/B/C: 2/2/1 powder blends MA'd for 2 h: (a) bright-field image, (b) dark-field image, (c) selected area diffraction pattern revealing the presence of ZrC particles ranging in size between 50 and 200 nm. Objective aperture is on (0 $\bar{2}$ 0), camera length is 100 cm and zone axis is [0 0 $\bar{1}$].

excess graphite is used in the mixture. It could be a constructive input for the properties of ZrB_2/ZrC ceramic powders but its investigation is not aimed in the scope of present study. In the current literature in which Zr/B/C: 4/2/3–6/10/1 powder mixtures are exposed to MA-SHS, it is not mentioned that some amount of Zr and C remain unreacted and some amount of B_4C phase forms, although it is unavoidable.[11,12]

In order to clearly understand the Zr–B–C ternary system, HSC Chemistry™ Ver. 4.1 and FactSage™ programs were used to calculate the reaction energetics. Gibbs free energy change versus temperature curves of the formation reactions of ZrB_2, ZrC and B_4C are respectively demonstrated in Fig. 4(a)–(c). The reactions have negative free energy changes which mean that they take place spontaneously and therefore they are thermodynamically feasible at temperatures between 25 and 2000 °C. Moreover, negative enthalpy changes of the reactions imply that an amount of heat is released during milling due to the exothermic reactions and the vial temperature increases significantly.[19] Fig. 4 also indicates that the formation of ZrB_2 is more preferential than ZrC and B_4C.

FactSage™ data, which is essential to comprehend the moles of probable products of the reactants in Zr–B–C system, are given in Table 1 for different mole ratios at room temperature. The results of the thermodynamic calculations show only the equilibrium phase composition at room temperature without considering synthesis history and reaction kinetics. Although the stoichiometric blend seems to be the most suitable one for preparing ZrB_2/ZrC ceramic powders according to Table 1, different mole ratios are tested using the unconventional MA method. Besides, the outputs are generally not in good

Table 1
Moles of probable products resulting from Zr–B–C reactions given in different mole ratios.

Zr/B/C mole ratio	Zr	B	C	ZrB_2	ZrC	B_4C
1/1/1	–	–	0.5	0.5	0.5	–
2/2/1	–	–	–	1	1	–
1/2/1	–	–	1	1	–	–
1/1/2	–	–	1.5	0.5	0.5	–
1/2/2	–	–	2	1	–	–

agreement with the XRD patterns of the MA'd Zr/B/C: 1/1/1, 1/2/1, 1/1/2 and 1/2/2 powder blends. Only the XRD pattern of the Zr/B/C: 2/2/1 powder blend MA'd for 2 h (Fig. 2(c)) matches quite well with the products mentioned in Table 1. Since the preferential formation is for ZrB_2, the formations of ZrC and B_4C and the presence of unreacted Zr are not taken into consideration in the thermodynamical data. Actually, MA process is related to the fracturing and welding mechanism and the contact points between the particles provide favourable conditions for the formation of the products. Due to the fact that MA process is far from equilibrium; synthesized phases are not expected to be compatible with thermodynamically calculated phases.

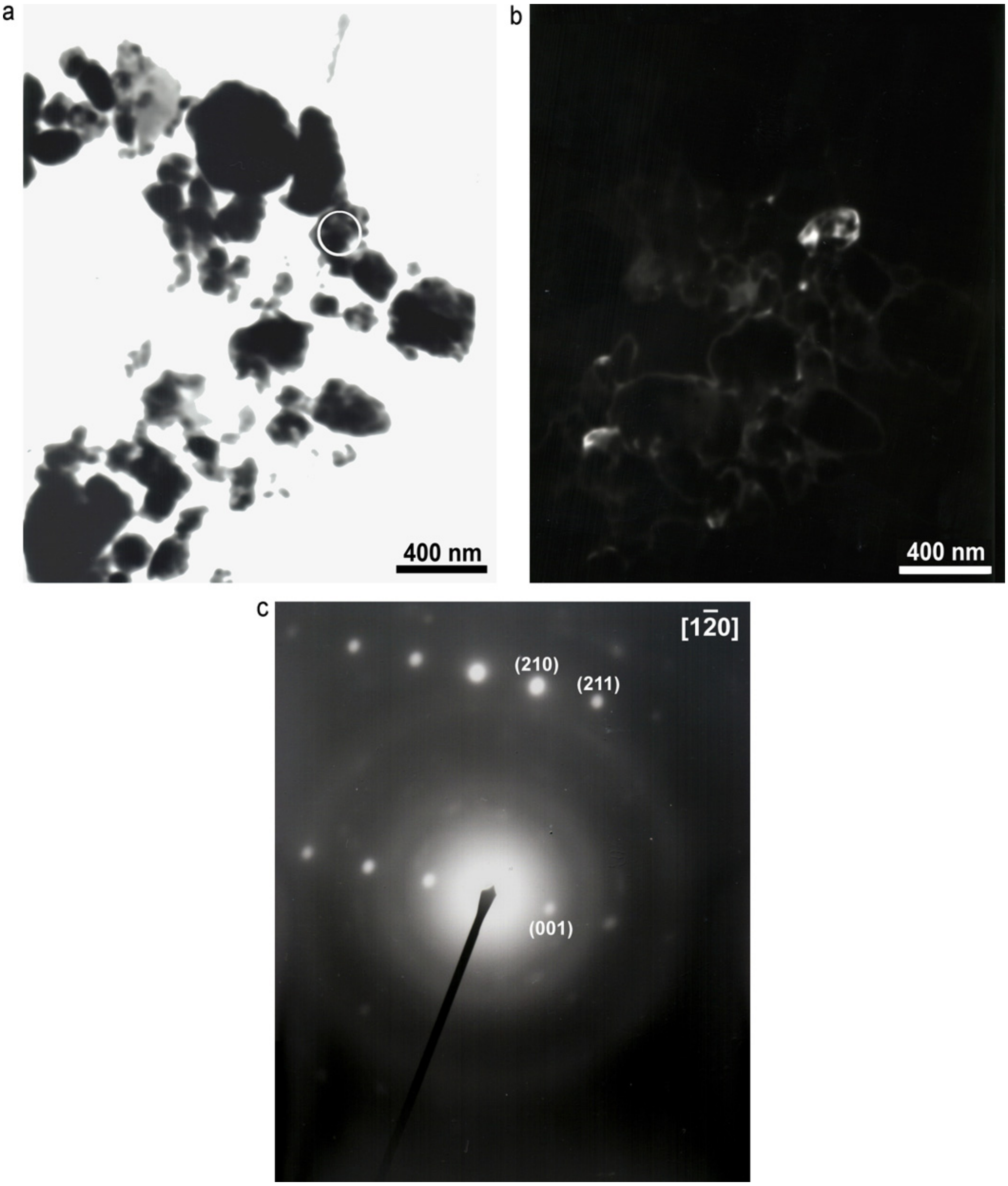

Fig. 9. TEM micrographs taken from Zr/B/C: 2/2/1 powder blends MA'd for 2 h: (a) bright-field image, (b) dark-field image, (c) selected area diffraction pattern revealing the presence of ZrB_2 particles ranging in size between 80 and 250 nm. Objective aperture is on $(0\,0\,\bar{1})$, camera length is 100 cm and zone axis is $[1\,\bar{2}\,0]$.

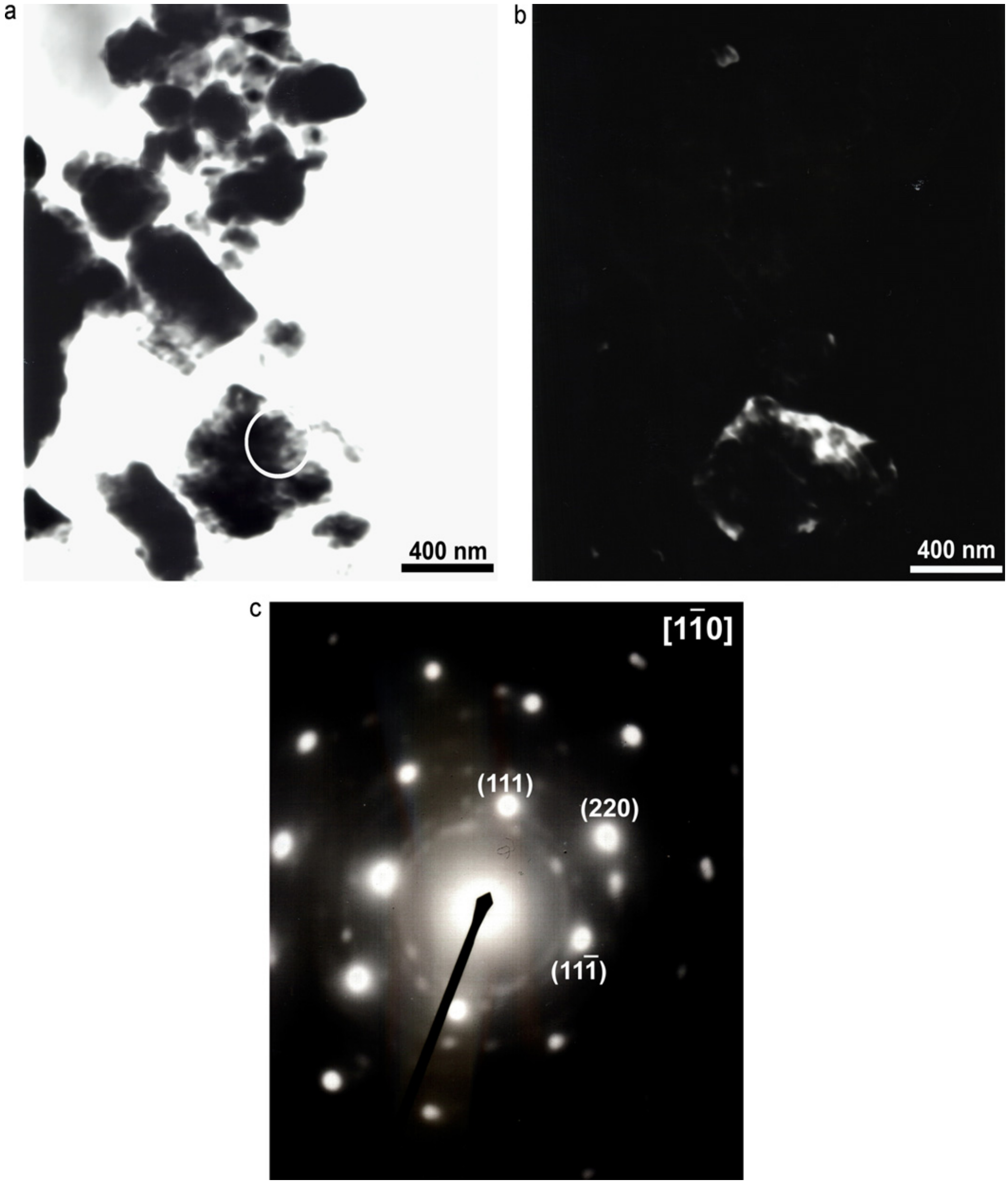

Fig. 10. TEM micrographs taken from Zr/B/C: 2/2/1 powder blends MA'd for 2 h: (a) bright-field image, (b): dark-field image, (c) selected area diffraction pattern revealing the presence of FeB particles ranging in size between 50 and 300 nm. Objective aperture is on $(\bar{1}\,\bar{1}\,\bar{1})$, camera length is 100 cm and zone axis is $[1\ \bar{1}\,0]$.

XRD patterns of the as-blended Zr/B/C: 2/2/1 powders heated to 800, 1000 and 1200 °C are respectively shown in Fig. 5(a)–(c). No reaction occurred between Zr, B and C powder particles until 1000 °C (Fig. 5(a) and (b)). However, Tsuchida and Yamamoto[10] have reported the formation of ZrB_2 at 800 °C and the formation of ZrC at 1000 °C after heating as-blended Zr/B/C: 1/1/1 powders for 1 h under Ar atmosphere. As seen in Fig. 5(c), after heating to 1200 °C, predominant formation of ZrB_2 and incubation of ZrC are detected in the presence of unreacted Zr and C phases. Depending on the heating temperature, the intensities of Zr peaks increase and sharpen due to the increase in crystallite size. The difference between initial particle sizes of raw materials and the excess amounts of Zr and C powders could affect the reaction mechanism and hence change the reaction temperature and products. The results in Fig. 5(a)–(c) indicate that if as-blended Zr/B/C: 2/2/1 powders are heated up to 1200 °C, an initial reaction between powder particles takes place to form very small amounts of ZrB_2 and ZrC phases. Mechanical activation is essential for the complete reaction without remaining unreacted Zr, B and C. The XRD patterns of the Zr/B/C: 2/2/1 powder blends MA'd for 2 h and heated to 800, 1000 and 1200 °C (Fig. 6(a)–(c)) also prove that there are no additional phases except ZrB_2 and ZrC.

Fig. 7(a) and (b) are the SEM images of the Zr/B/C: 2/2/1 powder blends MA'd for 2 h. As seen in these figures, powder mixtures consist of white and dark gray irregular agglomerates with sizes not larger than 500 nm. Although particle sizes are generally about 100 nm, agglomeration of the powder particles prevents the observation of smaller ones. Fig. 7(c) is a bright-field TEM image of Zr/B/C: 2/2/1 powder blends MA'd for 2 h showing irregular particles with a maximum size of 150 nm. On the basis of several EDS measurements taken from the mentioned regions in Fig. 7(b), white areas marked as ZrC contain about 86.38 ± 2.10 wt.% Zr and 13.62 ± 1.90 wt.% C and dark gray areas marked as ZrB_2 involve about 77.22 ± 3.63 wt.% Zr and 22.78 ± 3.62 wt.% B. EDS results are compatible with the calculated weight percentages of the elements in ZrB_2 and ZrC phases. EDS measurements are also supported by the XRD pattern in Fig. 2(c) indicating the presence of both ZrB_2 and ZrC phases following MA. Since a single powder particle does not contain both phases existing in the sampling volume, a ZrB_2/ZrC composite powder has not been formed.

Fig. 8(a) and (b) are the respective bright-field (BF) and dark-field (DF) TEM micrographs taken from the Zr/B/C: 2/2/1 powders MA'd for 2 h showing particles in size between 50 and 200 nm. Selected area diffraction pattern (SADP) taken from the white circled region in Fig. 8(a) is given in Fig. 8(c) and verifies the presence of ZrC particles. Fig. 9(a)–(c) are the respective BF, DF and SADP micrographs of ZrB_2 particles (between 80 and 250 nm) in the Zr/B/C: 2/2/1 powders MA'd for 2 h. SADPs indicate the areas marked with white circles in Figs. 9(a) and 10(a). Fig. 10(a)–(c) are a series of TEM micrographs (BF, DF and SADP) taken from the Zr/B/C: 2/2/1 powders MA'd 2 h, revealing FeB (ICDD Card No: 32-0463, Bravais lattice: primitive orthorhombic, $a = 0.406$ nm, $b = 0.55$ nm, $c = 0.295$ nm) particles in size between 50 and 300 nm. It is obvious that the FeB phase results from Fe contamination by the milling media (vial and balls). Gibbs free energy change versus temperature curve of the FeB formation reaction is demonstrated in Fig. 4(d). Although formation of FeB has negatively lower Gibbs free energy value (−60.353 kJ at 25 °C) than that of ZrB_2 (−318.238 kJ at 25 °C), the occurrence of FeB phase is unavoidable. Since the amount of Fe is not more than 1 wt.% of overall powder blend, it cannot be detected by XRD and SEM investigations unlike to ZrB_2 and ZrC particles. TEM micrographs cannot be utterly related to the literature findings because any study showing ZrB_2 and ZrC particles together in the same powder blend is accessible. However, Rangaraj et al.[14] and Shim et al.[20] have reported ZrB_2 and ZrC phases and phase boundaries in the ZrB_2/ZrC composites produced by reactive hot pressing and spark plasma sintering. Conversely, the presented research shows the formation of FeB contamination and the comparison of MA process with equilibrium predictions.

4. Conclusions

Based on the results of the present study, the following conclusions can be drawn:

(1) Mechanical alloying can be successfully utilized in the fabrication of ZrB_2/ZrC ceramic powders with fine microstructure as precursors of composites.
(2) The best result for the ZrB_2/ZrC ceramic powder was obtained from Zr/B/C: 2/2/1 powder blend mechanically alloyed for 2 h. In addition, FeB phase was determined in the TEM micrographs due to Fe contamination of powder particles.
(3) Zr/B/C: 1/1/1, 1/2/1, 1/1/2 and 1/2/2 powder blends mechanically alloyed for 2 and 3 h contain unreacted Zr and C ZrB_2 ZrC and B_4C particles.
(4) Zr/B/C: 2/2/1 powders mechanically alloyed for 2 h have ZrC particles in size between 50 and 200 nm, ZrB_2 particles in size between 80 and 250 nm and FeB particles in size between 50 and 300 nm.

Acknowledgements

We would like to express our gratitude to State Planning Organization (DPT) for funding the projects entitled "Advanced Technologies in Engineering" with the project number 2001K120750 and "Development of Al–Cu Based Metal Matrix Composites via Powder Metallurgy Techniques" with the project number 90189 out of which the main infrastructure of the Particulate Materials Laboratories was founded. Further, we would like to express our appreciations to Aziz Genç for his help in TEM analyses.

References

1. Radev DD, Klissurski D. Mechanochemical synthesis and SHS of diborides of titanium and zirconium. *Journal of Materials Synthesis and Processing* 2001;**9**:131–6.
2. Setoudeh N, Welham NJ. Formation of zirconium diboride (ZrB_2) by room temperature mechanochemical reaction between ZrO_2, B_2O_3 and Mg. *Journal of Alloys and Compounds* 2006;**420**:225–8.
3. Parthasarathy TA, Rapp RA, Opeka M, Kerans RJ. A model for the oxidation of ZrB_2 HfB_2 and TiB_2. *Acta Materialia* 2007;**55**:5999–6010.
4. Khanra AK. Reaction chemistry during self-propagating high-temperature synthesis (SHS) of H_3BO_3–ZrO_2–Mg system. *Materials Research Bulletin* 2007;**42**:2224–9.
5. Khanra AK, Pathak LC, Godkhindi MM. Double SHS of ZrB_2 powder. *Journal of Materials Processing Technology* 2008;**202**:386–90.
6. Shumilova RG, Kosolapova TY. Production of zirconium carbide on a pilot-plant scale. *Powder Metallurgy and Metal Ceramics* 1968;**7**:317–9.
7. Yan Y, Huang Z, Liu X, Jiang D. Carbothermal synthesis of ultra-fine zirconium carbide powders using inorganic precursors via sol–gel method. *Journal of Sol–Gel Science and Technology* 2007;**44**:81–5.
8. El-Eskandarany MS. *Mechanical alloying for fabrication of advanced engineering materials*. New York: Noyes Publications; 2001.
9. Tsuchida T, Yamamoto S, MA-SHS. SPS of ZrB_2–ZrC composites. *Solid State Ionics* 2004;**172**:215–6.
10. Tsuchida T, Yamamoto S. Mechanical activation assisted self-propagating high-temperature synthesis of ZrC and ZrB_2 in air from Zr/B/C powder mixtures. *Journal of the European Ceramic Society* 2004;**24**:45–51.
11. Tsuchida T, Yamamoto S. Spark plasma sintering of ZrB_2–ZrC powder mixtures synthesized by MA-SHS in air. *Journal of Materials Science* 2007;**42**:772–8.
12. Yan YJ, Zhang H, Huang ZR, Liu XJ, Dong SM. Synthesis of ultra-fine ZrB_2–ZrC composite powders by inorganic sol–gel method. *Journal of Inorganic Materials* 2008;**23**:815–8.
13. Guo WM, Zhang GJ. Microstructures and mechanical properties of hot-pressed ZrB_2-based ceramics from synthesized ZrB_2 and ZrB_2–ZrC powders. *Advanced Engineering Materials* 2009;**11**:206–10.
14. Rangaraj L, Suresha SJ, Divakar C, Jayaram V. Low-temperature processing of ZrB_2–ZrC composites by reactive hot pressing. *Metallurgical and Materials Transactions A* 2008;**39A**:1496–505.
15. Goutier F, Trolliard G, Valette S, Maître A, Estournes C. Role of impurities on the spark plasma sintering of ZrC_x–ZrB_2 composites. *Journal of the European Ceramic Society* 2008;**28**:671–8.
16. Guo SQ. Densification of ZrB_2-based composites and their mechanical and physical properties: a review. *Journal of the European Ceramic Society* 2009;**29**:995–1011.

17. Woo SK, Kim CH, Kang ES. Fabrication and microstructural evaluation of ZrB_2/ZrC/Zr composites by liquid infiltration. *Journal of Materials Science* 1994;**29**:5309–15.
18. Suryanarayana C. Mechanical alloying and milling. *Progress in Materials Science* 2001;**46**:1–184.
19. Murty BS, Ranganathan R. Novel materials synthesis by mechanical alloying/milling. *International Materials Reviews* 1998;**43**:101–41.
20. Shim SH, Niihara K, Auh KH, Shim KB. Crystallographic orientation of ZrB_2–ZrC composites manufactured by the spark plasma sintering method. *Journal of Microscopy* 2002;**205**:238–44.